Hydrogen Stark Broadening by Model Electronic Microfields

Joachim Seidel

Institut für Theoretische Physik der Universität Düsseldorf

(Z. Naturforsch. **32 a**, 1195–1206 [1977]; received July 21, 1977)

The Method of Model Microfields proposed by Brissaud and Frisch is applied to calculate Stark broadened profiles of hydrogen lines in the static ion approximation. Numerical results for L-α, H-α, and H-β are found to be in good agreement with those derived from the unified theory by Vidal, Cooper, and Smith over a wide range of plasma densities and temperatures. This demonstrates that reliable line profiles may be obtained from the microfield distribution and covariance alone, more complicated statistical features being less important in this context.

Generalizing a similar approach to magnetic resonance spectra [1, 2], Brissaud and Frisch [3, 4] have proposed the Method of Model Microfields (MMM) as a means to calculate the profiles of Stark broadened spectral lines emitted from a plasma. More recently, Brissaud et al.[5] have reexamined the validity of the method emphasizing its advantages. Nevertheless the MMM has found but few applications [3, 6] which deal solely with line profiles involving only a small number of atomic states, while a detailed MMM investigation of Stark broadened hydrogen lines is missing up to now. This seems to be due mainly to the fact that it is difficult to get reliable error estimates for the method since no systematic way of improvement is known at present from which these might deduced.

There are, of course, reasons substantiating the MMM's admissibility [3–5]: It works for a simple plasma-atom model, and yields correct results in the impact as well as the quasistatic limit. Still there remain doubts with regard to the correct description of the transition region between these two limiting cases. At least for the hydrogen lines, however, such doubts may be refuted by comparing the MMM results to those of the "unified theory" which has been elaborated by Voslamber [7] and Smith et al.[8] for the very purpose of describing the transition region for the broadening by plasma electrons. Extensive tables of hydrogen line profiles obtained with the help of this theory have been compiled by Vidal, Cooper, and Smith [9] (VCS), and within the frame of fundamental assumptions used by the unified theory (including especially the static ion approximation) these are the most reliable theoretical data available for a great range of plasma densities and temperatures. Therefore it is the aim of the present paper to show that the MMM yields profiles in close agreement with those of the unified theory if it starts from essentially the same presumptions. This will demonstrate most clearly the reliability of the MMM and provide a sound foundation for further applications.

Reprint requests to Dr. J. Seidel, Institut für Theoretische Physik der Universität Düsseldorf, Universitätsstraße 1, *D-4000 Düsseldorf*.

Section 1 contains a rather detailed review of the MMM in general, pointing out all approximations necessary to gain a form accessible to numerical evaluation. In Sect. 2 we consider the special case of hydrogen lines, and in Sect. 3 the choice of the probability density and covariance of the model microfield is discussed. Section 4 then presents the results of numerical computations together with a comparison to the profiles originating from the unified theory. A summary may be found in Section 5. Two appendices contain some calculational items which would have blown up Sect. 2 unduly.

1. MMM Review

We start in the usual way by expressing the unnormalized line profile as the Fourier transform of the autocorrelation function of the atomic dipole moment [10–12]:

$$J(\omega) = \frac{1}{2\pi} \int_{-\infty}^{\infty} \mathrm{d}t \exp\{i\omega t\} \operatorname{Tr} \boldsymbol{d} \cdot \langle T^{(\nu)\dagger}(t)\, \boldsymbol{d}\, T^{(n)}(t) \rangle . \tag{1.1}$$

We assume that the spectral line under consideration originates from an electrical dipole transition between a group of upper atomic states $\{|n\alpha\rangle\}$ and a group of lower states $\{|\nu\alpha\rangle\}$ spanning subspaces $\mathfrak{H}^{(n)}$ and $\mathfrak{H}^{(\nu)}$ of the full atomic state space. Then the trace in (1.1) is over these states. $\boldsymbol{d}$ is the operator of the atomic dipole moment, and $\langle \ldots \rangle$ indicates an average over the plasma-atom interaction.

$T^{(\nu)}(t)$ and $T^{(n)}(t)$ are the atomic evolution operators in the subspaces $\mathfrak{H}^{(\nu)}$ and $\mathfrak{H}^{(n)}$ which are assumed to be invariant during time evolution (no quenching approximation); $T^{(\nu)\dagger}$ is the Hermitian conjugate of $T^{(\nu)}$.

In "doubled atom" or "line space" tetradic notation [10] the normalized profile is

$$I(\omega) = \frac{1}{2\pi \operatorname{Tr} D} \int_{-\infty}^{\infty} \mathrm{d}t \exp\{i\omega t\} \operatorname{Tr} D \langle U(t) \rangle \quad (1.2)$$

with the operator

$$U(t) := T^{(n)}(t) \otimes T^{(\nu)*}(t) \quad (1.3)$$

working in the product space $\mathfrak{H}^{(n)} \otimes \mathfrak{H}^{(\nu)}$ (* denotes complex conjugation). The matrix elements of D between product states $|n a; \nu \alpha\rangle := |n a\rangle |\nu \alpha\rangle$ are defined as

$$\langle n a; \nu \alpha | D | n a'; \nu \alpha' \rangle : = \langle n a | \mathbf{d} | \nu \alpha \rangle \cdot \langle \nu \alpha' | \mathbf{d} | n a' \rangle , \quad (1.4)$$

and the trace in (1.2) is over these product states.

To get the equation of motion for $U(t)$ we confine ourselves to the dipole term $-\mathbf{d}\cdot\boldsymbol{E}(t)$ from the multipole expansion of the atom-plasma interaction. Then $U(t)$ must satisfy the Schrödinger equation

$$i\dot{U}(t) = \{[H_0^{(n)} - \mathbf{d}^{(n)}\cdot\boldsymbol{E}(t)] \otimes 1^{(\nu)} - 1^{(n)} \otimes [H_0^{(\nu)} - \mathbf{d}^{(\nu)}\cdot\boldsymbol{E}(t)]^*\} U(t) \quad (1.5)$$

with $U(0) = 1^{(n)} \otimes 1^{(\nu)}$ as initial condition. $H_0^{(n)}$ and $H_0^{(\nu)}$ are the restrictions to $\mathfrak{H}^{(n)}$ and $\mathfrak{H}^{(\nu)}$ of the unperturbed atomic Hamiltonian (likewise for $\mathbf{d}$ and the identity operator 1), and we use atomic units with $\hbar = 1$. Furthermore we treat the plasma as a classical system which is not at all influenced by the presence of the atom (classical path approximation [13]). By this assumption the plasma microfield $\boldsymbol{E}(t)$ becomes independent of $U(t)$ and may be regarded as a prescribed (though unknown) function of time in (1.5).

At this point it must be mentioned that we have tacitly introduced another standard approximation. To make it transparent let us describe the atom as a classical point particle with respect to its translational motion. Leaving out all complications from perturber-atom collisions [14], the atom has a nonvanishing thermal velocity in general. In the first instance this gives rise to the well known Doppler broadening of the spectral line. But in addition to this the microfield entering (1.5) depends on this velocity as well since $\boldsymbol{E}(t)$ has to be taken at the atomic position at time t. Hence there is a coupling of Stark and Doppler broadening, and the usual folding of the pertinent profiles is not rigorously exact. The unified theory accomplishes the decoupling of these broadening mechanisms by using the isotropic Maxwell distribution of perturber velocities in the observer's rest frame instead of the correct distribution of perturber-atom relative velocities. For electron perturbers the error introduced will usually be negligible because of the small ratio of atomic versus electronic thermal velocities. For ion perturbers, on the other hand, radiator motion cannot be omitted if ion motion is considered at all [12]. We need not, however, pursue this question any further here since for the present purpose the static ion approximation of the unified theory will be applied.

The problem left is to find the mean $\langle U(t) \rangle$ from the statistical properties of the plasma microfield. Due to the multiplicative appearance of $\boldsymbol{E}(t)$ in (1.5) it is necessary to have complete knowledge of the stochastic process $\boldsymbol{E}(t)$ to obtain the exact solution. Averaging the Neumann series solution of (1.5), for instance, it is immediately found that all many time moments of $\boldsymbol{E}(t)$ contribute to $\langle U(t) \rangle$. For this reason it is impossible to solve (1.5) with the true plasma microfield, and another approximation becomes inevitable. The unified theory retraces the field statistics to those of the perturbers, and approximates these in a suitable manner [15]. Contrary to this, the MMM intends to approximate the field statistics themselves retaining those features which are most important for the line profile. Up to now no quantitative argument is available which allows to evaluate the relative importance of the various statistical characteristics of the microfield in this context. Therefore it is impossible to ascertain the validity of the MMM without comparing its results to those of a well established theory as the present work will do for hydrogen lines.

Even if we cannot prove that only the most basic statistical features of the microfield bear markedly on the line profile, there is strong support to this assumption. For the electron broadening of hydrogen lines it is well known [10–12] that the line wing (or equivalently the short time behaviour of $\langle U(t) \rangle$) is determined by the microfield probability density while the line centre (long time behaviour of $\langle U(t) \rangle$) may be obtained from the microfield covariance. Hence any model which is supposed to

produce a reliable profile in both limiting cases has to retain these properties of the real microfield. Moreover it should ascribe to every value of the fieldstrength its true duration as correct as possible to ensure, for example, the essentially static action of strong fields. This may be effected by choosing a model which reproduces the conditioned covariance (with $\boldsymbol{E}(0) = \boldsymbol{E}$ held fixed) of the true microfield,

$$\gamma(t|\boldsymbol{E}) := \langle \boldsymbol{E}(t) \cdot \boldsymbol{E}(0) \rangle_{\boldsymbol{E}(0)=\boldsymbol{E}}, \qquad (1.6)$$

instead of just the usual unconditioned covariance $\langle \boldsymbol{E}(t) \cdot \boldsymbol{E}(0) \rangle$.

A model microfield which meets these requirements and at the same time makes the exact computation of $\langle U(t) \rangle$ feasible is most easily described by construction [4, 16]: Let $P(\boldsymbol{E})$ and $Q(\boldsymbol{E})$ be fieldstrength probability density functions (pdfs), and $w(t|\boldsymbol{E})$ and $v(t|\boldsymbol{E})$ pdfs with respect to t depending on $\boldsymbol{E}$ as a parameter. Choose fieldstrengths $\boldsymbol{E}_0$, $\boldsymbol{E}_1$, $\boldsymbol{E}_2$, ... independently of one another, $\boldsymbol{E}_0$ according to $P(\boldsymbol{E}_0)$, and $\boldsymbol{E}_1$, $\boldsymbol{E}_2$, ... according to $Q(\boldsymbol{E}_1)$, $Q(\boldsymbol{E}_2)$, ..., as well as successive instants of time $t_0, t_1, t_2, \ldots$ such that t_0 and the increments $t_1 - t_0$, $t_2 - t_1$, ... are independent and have pdfs $w(t_0|\boldsymbol{E}_0)$ and $v(t_1 - t_0|\boldsymbol{E}_1)$, $v(t_2 - t_1|\boldsymbol{E}_2)$, ..., respectively. Then

$$\boldsymbol{E}(t) = \begin{cases} \boldsymbol{E}_0, & 0 \leqq t < t_0 \\ \boldsymbol{E}_1, & t_0 \leqq t < t_1 \\ \boldsymbol{E}_2, & t_1 \leqq t < t_2 \\ \vdots \end{cases} \qquad (1.7)$$

is a realization of the stochastic model microfield which we shall call a "renewal process" because of the way the instants of time $t_0, t_1, t_2, \ldots$ have been selected [17]. In order to make this process stationary in time with pdf $P(\boldsymbol{E})$ we have to set

$$\begin{aligned} Q(\boldsymbol{E}) &= w(0|\boldsymbol{E})\, P(\boldsymbol{E}) / \langle w(0|E) \rangle_s, \\ v(t|\boldsymbol{E}) &= -\dot{w}(t|\boldsymbol{E}) / w(0|\boldsymbol{E}), \end{aligned} \qquad (1.8)$$

with the "static average" $\langle \ldots \rangle_s$ defined to be

$$\langle \ldots \rangle_s := \int \mathrm{d}^3E \ldots P(\boldsymbol{E}). \qquad (1.9)$$

Since $w(t|\boldsymbol{E})$ is closely related to the conditional covariance $\gamma(t|\boldsymbol{E})$ of this process,

$$\gamma(t|\boldsymbol{E}) = E^2 \int_t^\infty \mathrm{d}s\, w(s|\boldsymbol{E}), \qquad (1.10)$$

it may be stated that the statistics of a stationary renewal process are completely determined by its pdf $P(\boldsymbol{E})$ together with the conditional covariance $\gamma(t|\boldsymbol{E})$. If these are the corresponding quantities of the true microfield we may as well imagine that the renewal process has been obtained from the plasma microfield by approximating the statistical properties of the latter in the appropriate way. Clearly there is an infinite number of other ways this may be done. According to the fundamental assumption of the MMM, however, the line profile should be rather insensitive to the special features of the model used as long as this adheres to P and γ. Moreover, the renewal process just constructed is the only model known today for which the exact expression for the line profile has been obtained. Denoting the Laplace transform of the evolution operator by

$$\tilde{U}(\omega) := \int_0^\infty \mathrm{d}t \exp\{i\omega t\}\, U(t), \qquad (1.11)$$

we find from (1.5) with $\boldsymbol{E}(t)$ as given by (1.7) [4, 16]:

$$\begin{aligned} \langle \tilde{U}(\omega) \rangle_{\mathrm{MMM}} = & \int_0^\infty \mathrm{d}t \exp\{i\omega t\} \\ & \cdot \int_t^\infty \mathrm{d}s \langle w(s|\boldsymbol{E})\, U(t|\boldsymbol{E}) \rangle_s \\ & + \int_0^\infty \mathrm{d}t \exp\{i\omega t\} \langle w(t|\boldsymbol{E})\, U(t|\boldsymbol{E}) \rangle_s \\ & \cdot [\langle w(0|\boldsymbol{E}) \rangle_s + \int_0^\infty \mathrm{d}t \exp\{i\omega t\} \\ & \cdot \langle \dot{w}(t|\boldsymbol{E})\, U(t|\boldsymbol{E}) \rangle_s]^{-1} \\ & \cdot \int_0^\infty \mathrm{d}t \exp\{i\omega t\} \langle w(t|\boldsymbol{E})\, U(t|\boldsymbol{E}) \rangle_s . \end{aligned} \qquad (1.12)$$

Here $U(t|\boldsymbol{E})$ denotes the solution of (1.5) with static $\boldsymbol{E}(t) = \boldsymbol{E}$, i. e. an ordinary (non time ordered) exponential. Because of $\langle U(-t) \rangle = \langle U(t) \rangle^*$ the Fourier transform of $\langle U(t) \rangle$ in (1.2) is just $2 \cdot \mathrm{Re}\, \langle \tilde{U}(\omega) \rangle$, so the MMM profile ensues from the insertion of (1.12) into (1.2).

The general version of the MMM presented hitherto expresses the line profile in terms of the conditional covariance $\gamma(t|\boldsymbol{E})$, but actually this is not known for the true microfield. Therefore we have to introduce another approximation by making a guess on the form of γ or, equivalently, w. With a view to the Laplace transforms to be done in (1.12) a convenient choice is

$$w(t|\boldsymbol{E}) = v(t|\boldsymbol{E}) = \Omega(\boldsymbol{E}) \exp\{-\Omega(\boldsymbol{E})t\}, \qquad (1.13)$$

which assigns a familiar exponential decay to γ, but still leaves the determination of the mean duration $\Omega^{-1}(\boldsymbol{E})$ for the various fieldstrengths. This may be

accomplished by setting the unconditioned covariance $\Gamma(t)$ of the model field equal to that of the real microfield since Γ and Ω are connected through

$$\Gamma(t) := \langle \gamma(t|\boldsymbol{E}) \rangle_s = \int \mathrm{d}^3E\, E^2 \exp\{-\Omega(\boldsymbol{E})t\}\, P(\boldsymbol{E})\,. \tag{1.14}$$

Contrary to γ, Γ is reasonably well known from plasma kinetic theory [18] (yet we shall be content with a rough form derived from a simple plasma model for the numerical calculations, see section 3).

For an isotropic microfield Ω and P depend on the modulus E of $\boldsymbol{E}$ only. Then, under the extra assumption of an everywhere increasing $\Omega(E)$ tending to infinity with E, the right hand side of (1.14) is essentially a Laplace transform which has to be inverted to obtain Ω from Γ. The special Markovian version (1.13) of the general renewal process is the "kangaroo process" originally introduced by Brissaud and Frisch [3] and subsequently applied to simple line profiles by Brissaud et al. [6]. In what follows we, too, shall exclusively use this model for which the fundamental formula (1.12) simplifies to

$$\begin{aligned}\langle \tilde{U}(\omega) \rangle_{\mathrm{MMM}} = {} & \langle \tilde{U}(\omega'|\boldsymbol{E}) \rangle_s + \langle \Omega(\boldsymbol{E})\, \tilde{U}(\omega'|\boldsymbol{E}) \rangle_s \\ & \cdot [\langle \Omega(\boldsymbol{E}) \rangle_s - \langle \Omega^2(\boldsymbol{E})\, \tilde{U}(\omega'|\boldsymbol{E}) \rangle_s]^{-1} \\ & \cdot \langle \Omega(\boldsymbol{E})\, \tilde{U}(\omega'|\boldsymbol{E}) \rangle_s\,, \end{aligned} \tag{1.15}$$

the Laplace transform being taken at $\omega' := \omega + i\,\Omega(\boldsymbol{E})$.

For the sake of transparency we have pretended till now that a single covariance Γ is well suited to describe the time correlation of the plasma microfield. Evidently this fits reality but poorly, because the microfield consists of a high frequent "electronic" part and a low frequent "ionic" part with very different correlation times. The appropriate model for this case is the superposition of a slow ionic renewal process with a fast electronic process [3], characterized by subscripts i and e. To get the line profile for the compound process we have to compute first the electronic mean of the evolution operator with $\boldsymbol{E}_\mathrm{i}$ held fixed, and then use this instead of $U(t|\boldsymbol{E})$ in (1.12). For Markovian kangaroo processes the first step results in

$$\begin{aligned}\tilde{U}_\mathrm{i}(\omega|\boldsymbol{E}_\mathrm{i}) = {} & \langle \tilde{U}(\omega_\mathrm{e}'|\boldsymbol{E}_\mathrm{i}+\boldsymbol{E}_e) \rangle_\mathrm{e} \\ & + \langle \Omega_\mathrm{e}(\boldsymbol{E}_\mathrm{e})\, \tilde{U}(\omega_\mathrm{e}'|\boldsymbol{E}_\mathrm{i}+\boldsymbol{E}_\mathrm{e}) \rangle_\mathrm{e} \\ & \cdot [\langle \Omega_\mathrm{e}(\boldsymbol{E}_\mathrm{e}) \rangle_\mathrm{e} - \langle \Omega_\mathrm{e}^2(\boldsymbol{E}_\mathrm{e}) \\ & \cdot \tilde{U}(\omega_\mathrm{e}'|\boldsymbol{E}_\mathrm{i}+\boldsymbol{E}_\mathrm{e}) \rangle_\mathrm{e}]^{-1} \\ & \cdot \langle \Omega_\mathrm{e}(\boldsymbol{E}_\mathrm{e})\, \tilde{U}(\omega_\mathrm{e}'|\boldsymbol{E}_\mathrm{i}+\boldsymbol{E}_\mathrm{e}) \rangle_\mathrm{e}\,, \end{aligned} \tag{1.16}$$

and finally we get

$$\begin{aligned}\langle \tilde{U}(\omega) \rangle_{\mathrm{MMM}} = {} & \langle \tilde{U}_\mathrm{i}(\omega_\mathrm{i}'|\boldsymbol{E}_\mathrm{i}) \rangle_\mathrm{i} \\ & + \langle \Omega_\mathrm{i}(\boldsymbol{E}_\mathrm{i})\, \tilde{U}_\mathrm{i}(\omega_\mathrm{i}'|\boldsymbol{E}_\mathrm{i}) \rangle_\mathrm{i} \\ & \cdot [\langle \Omega_\mathrm{i}(\boldsymbol{E}_\mathrm{i}) \rangle_\mathrm{i} - \langle \Omega_\mathrm{i}^2(\boldsymbol{E}_\mathrm{i}) \\ & \cdot \tilde{U}_\mathrm{i}(\omega_\mathrm{i}'|\boldsymbol{E}_\mathrm{i}) \rangle_\mathrm{i}]^{-1} \\ & \cdot \langle \Omega_\mathrm{i}(\boldsymbol{E}_\mathrm{i})\, \tilde{U}_\mathrm{i}(\omega_\mathrm{i}'|\boldsymbol{E}_\mathrm{i}) \rangle_\mathrm{i}\,, \end{aligned} \tag{1.17}$$

the static averages $\langle \ldots \rangle_\mathrm{e}$ and $\langle \ldots \rangle_\mathrm{i}$ taken according to $P_\mathrm{e}(\boldsymbol{E}_\mathrm{e})$ and $P_\mathrm{i}(\boldsymbol{E}_\mathrm{i})$ and ω_e' and ω_i' defined as $\omega'_{\mathrm{e,i}} := \omega + i\,\Omega_{\mathrm{e,i}}(\boldsymbol{E}_{\mathrm{e,i}})$.

(1.16) and (1.17) show clearly that the MMM takes into account the time dependence of the ionic part of the microfield in exactly the same way as that of the electronic part. Hence, using the MMM it is not necessary to make the static ion assumption which is an essential ingredient of the unified theory. For this reason the method is perfectly suited to investigate the influence of ion motion on spectral line profiles. But at present we are merely interested in a comparison of the MMM to the unified theory, so we neglect the time dependence of the ionic field by taking the limit $\Omega_\mathrm{i} \to 0$ in (1.17). Then the second summand of the right hand side vanishes, and the line shape results from the usual superposition of electron broadened profiles split in the constant field $\boldsymbol{E}_\mathrm{i}$.

2. Application to Hydrogen

We shall now sketch the evaluation of the rather compact formulas (1.16) and (1.17) for the case of hydrogen lines. Choosing upper and lower states to be those with principal quantum numbers n and ν we have

$$H_0^{(n)} \otimes 1^{(\nu)} - 1^{(n)} \otimes H_0^{(\nu)} = \omega_{n\nu}\, 1^{(n)} \otimes 1^{(\nu)} \tag{2.1}$$

in (1.5), where $\omega_{n\nu}$ is the frequency of the sharp unperturbed line (we use atomic units, especially $\hbar = 1$, and neglect the natural line width as well as fine structure splitting). It is advantageous to split off the corresponding oscillation from U:

$$U(t|\boldsymbol{E}) =: \exp\{-i\,\omega_{n\nu}\,t\}\, W(t|\boldsymbol{E}), \tag{2.2}$$

and to use the frequency difference

$$\Delta\omega := \omega - \omega_{n\nu} \tag{2.3}$$

instead of ω. The unitary operator W describes the effect of the electric field on time evolution in line space:

$$W(t\,|\,\boldsymbol{E}_\mathrm{i}+\boldsymbol{E}_\mathrm{e}) \tag{2.4}$$
$$=\exp\{-i\,t(\boldsymbol{E}_\mathrm{i}+\boldsymbol{E}_\mathrm{e})\cdot(\boldsymbol{r}^{(n)}\otimes 1^{(\nu)}-1^{(n)}\otimes r^{(\nu)*})\}$$
$$=\exp\{-i\,t(\boldsymbol{E}_\mathrm{i}+\boldsymbol{E}_\mathrm{e})\cdot\boldsymbol{r}^{(n)}\}\otimes\exp\{i\,t(\boldsymbol{E}_\mathrm{i}+\boldsymbol{E}_\mathrm{e})\cdot\boldsymbol{r}^{(\nu)*}\}$$

(in atomic units, $\boldsymbol{d}=-\boldsymbol{r}$ with $\boldsymbol{r}$ the operator of the electron's position relative to the atomic nucleus).

Now let $\boldsymbol{E}_\mathrm{i}$ be specified by its modulus E_i and polar angles Θ_i, Φ_i with respect to some fixed system of coordinates, and $\boldsymbol{E}_\mathrm{e}$ by E_e, the angle Θ_e it forms with $\boldsymbol{E}_\mathrm{i}$, and the azimuth Φ_e in a plane perpendicular to $\boldsymbol{E}_\mathrm{i}$. Then the first factor of W is

$$\exp\{-i\,t(\boldsymbol{E}_i+\boldsymbol{E}_\mathrm{e})\cdot\boldsymbol{r}^{(n)}\}=R^{(n)}(\Phi_\mathrm{i},\Theta_\mathrm{i},\Phi_\mathrm{e})$$
$$\cdot\exp\{-i\,t\boldsymbol{E}\cdot\boldsymbol{r}^{(n)}\}\,R^{(n)\dagger}(\Phi_\mathrm{i},\Theta_\mathrm{i},\Phi_\mathrm{e})\,, \tag{2.5}$$

with the unitary rotation operator

$$R^{(n)}(\Phi_\mathrm{i},\Theta_\mathrm{i},\Phi_\mathrm{e}):=\exp\{-i\,\Phi_\mathrm{i}\,l_z^{(n)}\}$$
$$\cdot\exp\{-i\,\Theta_\mathrm{i}\,l_y^{(n)}\}\exp\{-i\,\Phi_\mathrm{e}\,l_z^{(n)}\} \tag{2.6}$$

and the rotated electric field

$$\boldsymbol{E}:=\boldsymbol{e}_x E_\mathrm{e}\sin\Theta_\mathrm{e}+\boldsymbol{e}_z(E_\mathrm{i}+E_\mathrm{e}\cos\Theta_\mathrm{e})\,. \tag{2.7}$$

The rotation operators are most conveniently handled in a basis of angular momentum eigenstates, so we take the well-known "spherical" states $|n\,l\,m\rangle$ and $|\nu\,\lambda\,\mu\rangle$ as base vectors in $\mathfrak{H}^{(n)}$ and $\mathfrak{H}^{(\nu)}$, and their products $|n\,l\,m;\nu\,\lambda\,\mu\rangle$ as base vectors in $\mathfrak{H}^{(n)}\otimes\mathfrak{H}^{(\nu)}$ (for brevity, we shall frequently drop n and ν). Then the matrices representing $x^{(\nu)}$ and $z^{(\nu)}$ are real while $y^{(\nu)}$ is purely imaginary [19]. Hence $(\boldsymbol{E}_\mathrm{i}+\boldsymbol{E}_\mathrm{e})\cdot\boldsymbol{r}^{(\nu)*}$ may be obtained from $(\boldsymbol{E}_\mathrm{i}+\boldsymbol{E}_\mathrm{e})\cdot\boldsymbol{r}^{(\nu)}$ by changing the signs of Φ_i and Φ_e:

$$\exp\{i\,t(\boldsymbol{E}_\mathrm{i}+\boldsymbol{E}_\mathrm{e})\cdot\boldsymbol{r}^{(\nu)*}\}=R^{(\nu)}(-\Phi_\mathrm{i},\Theta_\mathrm{i},-\Phi_\mathrm{e})$$
$$\cdot\exp\{i\,t\boldsymbol{E}\cdot\boldsymbol{r}^{(\nu)}\}\,R^{(\nu)\dagger}(-\Phi_\mathrm{i},\Theta_\mathrm{i},-\Phi_\mathrm{e})\,. \tag{2.8}$$

With the angular dependence of $U(t\,|\,\boldsymbol{E}_\mathrm{i}+\boldsymbol{E})$ made explicit in this way we may partly perform the static averages in (1.16) and (1.17). As we neglect any anisotropy due to radiator motion, the model microfield is isotropic with

$$P_\mathrm{e}(\boldsymbol{E}_\mathrm{e})=(4\pi E_\mathrm{e}^2)^{-1}P_\mathrm{e}(E_\mathrm{e})\,,\quad \Omega_\mathrm{e}(\boldsymbol{E}_\mathrm{e})=\Omega_\mathrm{e}(E_\mathrm{e})\,, \tag{2.9}$$

and the static average becomes

$$\langle\ldots\rangle_\mathrm{e}=\int_0^\infty \mathrm{d}E_\mathrm{e}\,P_\mathrm{e}(E_\mathrm{e})\cdot\frac{1}{2}\int_0^\pi \mathrm{d}\Theta_\mathrm{e}\sin\Theta_\mathrm{e}\cdot\frac{1}{2\pi}\int_0^{2\pi}\mathrm{d}\Phi_\mathrm{e}\ldots\,, \tag{2.10}$$

similar relations holding for P_i, Ω_i, and $\langle\ldots\rangle_\mathrm{i}$. Using this in (1.16), the directional average relates to $\tilde{U}(\omega_\mathrm{e}'\,|\,\boldsymbol{E}_\mathrm{i}+\boldsymbol{E}_\mathrm{e})$ only. Inserting (2.6) and (2.8) into (2.4), it is easily shown that the only non-vanishing matrix elements $\langle l\,m;\lambda\,\mu\,|\,\langle\tilde{U}(\omega_\mathrm{e}'\,|\,\boldsymbol{E}_\mathrm{i}+\boldsymbol{E}_\mathrm{e})\rangle_{\Phi_\mathrm{e}}\,|\,l'\,m';\lambda'\,\mu'\rangle$ are those with $m-\mu=m'-\mu'$. The same holds true for the matrix elements of $\langle\tilde{U}_\mathrm{i}(\omega_\mathrm{i}'\,|\,\boldsymbol{E}_\mathrm{i})\rangle_{\Theta_\mathrm{i},\Phi_\mathrm{i}}$, and these at last may be computed from those elements of $\tilde{U}_\mathrm{i}(\omega_\mathrm{i}'\,|\,E_\mathrm{i}\,\boldsymbol{e}_z)$ meeting the same condition (for a proof, see appendix A).

With this structure of the matrices involved we may reduce the numerical expenditure considerably by grouping the states $|l\,m;\lambda\,\mu\rangle$ according to the difference $a:=m-\mu$, numbering those with the same a by a second index. As a result of this rearrangement of the basis the matrix of $\langle\tilde{U}(\omega_\mathrm{e}'\,|\,\boldsymbol{E}_\mathrm{i}+\boldsymbol{E}_\mathrm{e})\rangle_{\Phi_\mathrm{e}}$ becomes block diagonal. Neither averaging nor inverting destroy this structure, so it is preserved for $\tilde{U}_\mathrm{i}$ and $\langle\tilde{U}\rangle_\mathrm{MMM}$ as well. For the numerics this is a distinct faciliation. Consider H-β as an example ($n=4$, $\nu=2$): a may take the values 0, $\pm1,\ldots,\pm4$, and there are 14 states with $a=0$, $16-4\,|\,a\,|$ states with $a=\pm1$, ±2, ±3, and one state for each $a=\pm4$. Accordingly, instead of all the $64^2=4096$ elements of any matrix, only those 646 with $a=a'$ have to be stored (further symmetry relations may be used to reduce this number still more), and the biggest matrix to be inverted is only 14×14, not 64×64.

The averages with respect to Φ_i, Θ_i, and Φ_e done, it is sufficient to consider an electric field of the special form given by (2.7), for which $\tilde{W}$ may be written in the form

$$\tilde{W}(\omega\,|\,\boldsymbol{E})=i\sum_{N,k}(\omega\,H_{2k,N}^{(n,\nu)}+\tfrac{3}{2}N\,E_z\,H_{2k+1,N}^{(n,\nu)})$$
$$\cdot\left(\omega^2-\frac{9\,N^2}{4}E^2\right)^{-1}(E_z/E)^{2k}$$
$$+\text{remainder}\,, \tag{2.11}$$

the Φ_e-average of the remainder vanishing. The $H_{k,N}^{(n,\nu)}$ are constant matrices characteristic for the line $n\rightarrow\nu$ which may be computed once and for all. The deduction of (2.11) is deferred to appendix B. With this form of $\tilde{W}$, it would even be possible to perform the Θ_e-average analytically (only E_z and E depend on Θ_e). However, the integrals encountered have to be calculated recursively, and this could not be done sufficiently accurate with the computer used. As an approximation proposed by Brissaud et al. [6] proved to be inaccurate for the case of hydrogen, too, the average has been computed numerically. The remaining integrations with respect to E_e and E_i have to be done numerically anyhow, if use is made of tabulated probability densities.

At last it may be worth mentioning that the static ion approximation renders both the Θ_i- and the Φ_i-average superfluous: the line profile given by (1.2) corresponds to the intensity of radiation averaged over all directions of emission, and is independent of the direction of $\boldsymbol{E}_i$ as long as this remains constant in time.

3. Model Field Distribution and Covariance

For the performance of the averages remaining in (1.16) and (1.17) knowledge is required of the probability densities $P_i(E_i)$ and $P_e(E_e)$ together with the jumping frequencies $\Omega_i(E_i)$ and $\Omega_e(E_e)$. As we want to apply the static ion approximation of the unified theory in the frame of the MMM as well, we set $\Omega_i(E_i) = 0$. The distribution functions of the low frequency microfield component we use are that given by Baranger and Mozer [20, 21] (with the corrections of numerical inaccuracies as given by Pfennig and Trefftz [22]) or Hooper [23, 24], which are nearly identical to one another. The same values have been used by VCS[9] in their evaluation of the unified theory.

It is more difficult to fix the quantities relating to the electronic part of the microfield. A well-known result from plasma kinetic theory expresses $\Gamma_e(t)$ in terms of the dielectric function [18, 25], and may be derived from a model plasma composed of noninteracting, dynamically shielded quasi-electrons. The use of this covariance in the MMM, however, would necessitate extensive numerical efforts. For this reason we prefer to retreat to a plasma model of uncorrelated quasi-particles with Debye type fields resulting from static screening. (In other line broadening calculations it is even usual practice to employ a Coulomb field with appropriate cutoff, but we need not do this here.) Denoting the screening length by R the covariance is found to be [5]

$$\Gamma_e(t) = 4\pi^{1/2} e^2 N_e R[s + s^{-1} - \pi^{1/2}(s^2 + \tfrac{3}{2}) \cdot \exp(s^2)\,\mathrm{erf}(s)]\,, \tag{3.1}$$

with the abbreviation $s := [kT_e/(2m_e)]^{1/2} \cdot t/R$. As $\Omega_e(t \to \infty) \sim t^{-5}$, we must take $\Omega_e(0) = 0$ in (1.14), and have

$$\int_0^\beta d\alpha\, \alpha^2 p_e(\alpha) = 2\pi^{-3/2}(15/4)^{4/3} R^{-1} N_e^{-1/3} \cdot \left[\frac{\Omega_e}{\omega_e} + \frac{1}{2}\frac{\Omega_e}{\omega_e}\exp\left(-\frac{\Omega_e^2}{\omega_e^2}\right) - \frac{3}{4}\pi^{1/2}\,\mathrm{erf}\left(\frac{\Omega_e}{\omega_e}\right)\right] \tag{3.2}$$

as the equation from which Ω_e has to be determined. In (3.2) we have used reduced fieldstrengths $\beta := E/E_0$ (the characteristic fieldstrength is $E_0 := 2\pi e(4/15)^{2/3} N_e^{2/3}$), their probability density $p_e(\beta) = E_0 P_e(\beta E_0)$, and the characteristic frequency ω_e defined by $\omega_e^2 := kT_e/(2m_e R^2)$. The numerical solution of (3.2) poses no problem if p_e is sufficiently well known.

For the probability density p_e we would like to take the values given by Baranger and Mozer [20, 22] or Hooper [23] as we have done for p_i. On the other hand, for consistency we should derive p_e from our plasma model. Fortunately enough, both these intentions may be effected by setting the screening length R equal to twice the Debye length,

$$R = 2D = 2[kT_e/(4\pi e^2 N_e)]^{1/2}\,. \tag{3.3}$$

The microfield distribution of the model plasma then turns out to be nearly identical to that of the above-mentioned authors over the relevant range of the plasma parameter. The exact value of R/D, however, is not very important in the present context as has been checked by computing some profiles with $R = D$ in place of (3.3) as well. This corresponds to a modification of the impact parameter cutoff in the unified theory, and causes about the same changes in the line profile: while the line centre may be altered by a few percent, the line wing is not affected. As the VCS profiles with which we want to compare our results are afflicted with similar uncertainties, we need not be concerned about this, and for the numerical computations have relied on (3.3).

Let us conclude this paragraph with an inspection of the lifetime of strong model fields. For $E_e \gg E_0$, $p_e(\beta)$ exhibits the asymptotic $\beta^{-5/2}$-dependence typical for point particles producing a Coulomb field in their immediate vicinity. Using this asymptotic form throughout, the integral in (3.2) may be estimated by $3\beta^{1/2}$. At the same time we may replace the right hand side by its leading term since we have $\Omega_e \to \infty$ for $E_e \to \infty$. The result for the mean duration of strong fields is

$$\Omega_e^{-1} \cong 1.1\,[e m_e/(kT_e)]^{1/2} E_e^{-1/2}\,. \tag{3.4}$$

It is consistent with the value one expects from the particle picture: Let E_e be due to a "nearest neighbour" with distance r from the test point and velocity v. The lifetime of the field effected by this particle is roughly $\tau \cong r/v$. Inserting the mean thermal velocity for v, and utilizing $E_e \cong e r^{-2}$, we

obtain $\tau \cong 0.6 \cdot [e\, m_e/(k\, T_e)]^{1/2} E_e^{-1/2}$. Therefore, the Markovian model microfield describes strong fields correctly. For weak fields the true duration is not known because they originate from the joint action of several electrons. A guess based on this collective nature could be $\tau \lesssim \omega_p^{-1}$ with the plasma frequency defined as usual, i. e. $\omega_p^2 = k\, T_e/(2\, m_e\, D^2) = 4\,\pi\, e^2\, N_e/m_e$. In consequence of $\Omega_e(0) = 0$ very weak fields last longer than this in the model. Their probability, however, is small as a closer inspection of (3.2) reveals, so they cannot cause great errors in the line profile.

4. Comparison of MMM and Unified Theory

The general MMM results for hydrogen lines have been evaluated for the Lyman line L-α and the first two members of the Balmer sequence, H-α and H-β. The numerical computation was done with the CDC Cyber 76 of the Regionalrechenzentrum Köln via the RJE-station of the Rechenzentrum der Universität Düsseldorf. As the computation times were not too long (from about one minute for L-α to five minutes for H-β) profiles of all three lines could be obtained for densities N ($N_e = N_i = N$ has been assumed) from 10^{15} to $10^{18}\,\mathrm{cm}^{-3}$ and electron temperatures T_e of 5000 K, 10 000 K, 20 000 K, and 40 000 K. With this great range of plasma conditions covered it becomes possible not only to compare single profiles to those of VCS, but to examine the density and temperature dependence of characteristic quantities such as peak intensities and fractional widths, too. This does obviously rule out the possibility of drawing conclusions from purely fortuitous coincidences.

The general result of the comparison of MMM and VCS profiles is that both yield nearly identical results, the MMM profiles exhibiting somewhat less structure in the line centre throughout. Figures 1 to 3 give typical examples of the three lines considered here for plasma conditions which are well within the range of validity of the unified theory ($T = 10^4$ K, $N = 3.2 \cdot 10^{16}\,\mathrm{cm}^{-3}$). In all three cases the MMM intensity, is slightly lower in the peak than that of the VCS profiles, becomes a little higher beyond the half width to maintain normalization (MMM as well as VCS profiles are automatically normalized to unit area). Further out in the line wing the profiles merge into one and become indistinguishable.

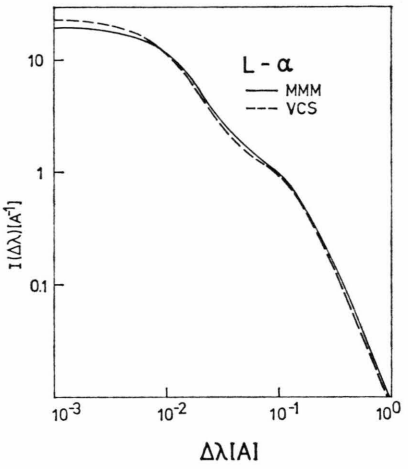

Fig. 1. Comparison of normalized L-α Stark profiles obtained from the MMM and the unified theory (VCS). Plasma conditions are $N = 3.2 \cdot 10^{16}\,\mathrm{cm}^{-3}$, $T = 10^4$ K.

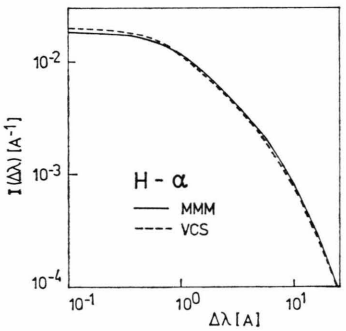

Fig. 2. Same as Fig. 1, but for H-α.

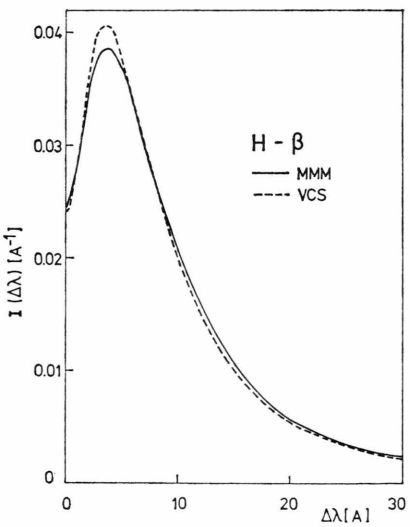

Fig. 3. Same as Fig. 1, but for H-β.

A still closer agreement in the line centre could be obtained by using a screening length smaller than $2D$. On the other hand it is well known that the VCS profiles are not quite correct in their central portions due to the neglect of time ordering in the calculation of the atomic evolution operator. (For the MMM this problem does not arise since it gives the exact line profile for the model microfield.) This approximation is not, however, substantial for the unified theory, and a recent investigation by Roszman [26] indicates that the proper inclusion of time ordering in the VCS calculations would reduce the structure of their line centres to approximately that of the MMM profiles or even somewhat more. With this in mind the agreement of the MMM and VCS profiles depicted in figures 1 to 3 appears still more perfect. The same holds true over the whole range of plasma densities and temperatures examined. In Fig. 4 the (full) half, quarter, and eighth widths of H-α are plotted as functions of the electron density for a plasma temperature of 10^4 K. The MMM curves lie about 10% higher than those of VCS, both are parallel and nearly straight lines (in this logarithmic representation) over all three decades of plasma density. For the half width, Roszman's data have been included which are even closer to the MMM results. A similar agreement is found for the temperature dependence of the fractional widths (Figure 5).

The corresponding curves for L-α and H-β coincide as well as those for H-α, and have been omitted for this reason. Instead, two special features of these lines are pictured. Figure 6 gives the peak intensity of L-α as a function of electron density; the relative difference of the MMM and VCS values is seen to be the same as that of Fig. 1 (about 10%) in the whole range. Contrary to L-α and H-α with their strong unshifted components in a static electric field, H-β has a characteristic depression in the line centre the strength of which is conveniently measured by the "dip" [27] defined as $(I_{\max}-I_{\min})/I_{\max}$, with $I_{\max}$ and $I_{\min}$ the maximal and the central intensity, respectively. The density dependence of this quantity is represented in Fig. 7, where again the MMM data lie well between those of VCS (unified theory without time ordering) and Roszman (unified theory with time ordering). As the VCS tables do not give H-β profiles for densities greater than 10^{17} cm^{-3}, the comparison cannot be extended to this range where the MMM

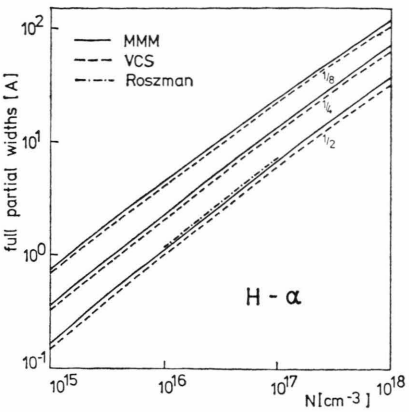

Fig. 4. Density dependence of H-α partial widths for $T=10^4$ K. Beside the results of the present work (MMM) and the unified theory without time ordering (VCS), the half width data given by Roszman (unified theory with time ordering) are shown.

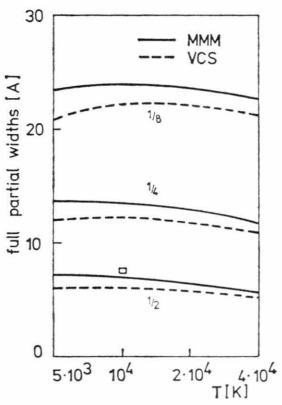

Fig. 5. Temperature dependence of H-α partial widths (Doppler broadening included) for $N=10^{17}$ cm^{-3}. The results of the present work (MMM) are compared to those of the unified theory without time ordering (VCS). The rectangle marks the half width value obtained by Roszman (unified theory including time ordering).

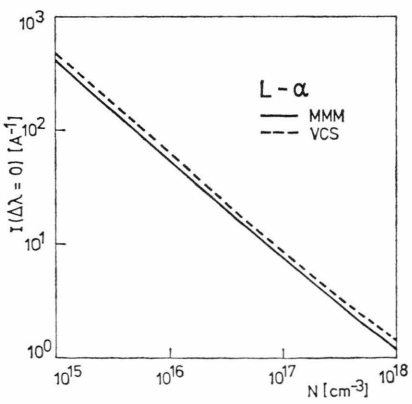

Fig. 6. Peak intensity of L-α (Stark broadening only) at $T=10^4$ K as a function of plasma density. The results of the MMM and the unified theory (VCS) are depicted.

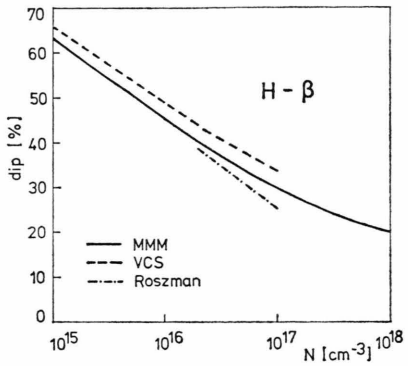

Fig. 7. The dip of H-β (Stark broadening only) as calculated by the MMM and the unified theory without (VCS) and with (Roszman) time ordering. The plasma temperature is $T=10^4$ K.

curve starts to deviate markedly from a straight line (the dip must remain positive by definition). For lower densities the agreement is excellent once more.

Taken together, the results presented here demonstrate most clearly that reliable line profiles may be obtained with the help of the MMM from the microfield distribution and covariance alone. For the unified theory this implies that actually all the details of atom-electron collisions entering the calculation bear on the line profile only to the extent to which they influence these basic statistical properties of the plasma microfield.

With the close accordance found there is no use in comparing the MMM results to experimental profiles. Wiese and coworkers [27, 28], for example, report good agreement of their precision measurements with the VCS profiles in the line wings, but surprisingly large differences in the line centre. The same holds true for the MMM profiles, of course, which here have been computed under the static ion approximation. For the MMM, however, it is possible to drop this approximation which cannot be done in the unified theory. This proper consideration of ion motion is expected to improve the agreement of theoretical predictions and experimental findings [27].

5. Conclusion

In order to establish its admissibility for the case of hydrogen lines, we have reviewed the MMM introduced by Brissaud and Frisch [3], and applied it to the calculation of electron broadening of the L-α, H-α, and H-β lines in the frame of the static ion approximation. An extensive comparison to the results of the unified theory obtained by Vidal, Cooper, and Smith [9] shows that both procedures are equivalent and the MMM yields not only the line centre and wing correctly but also the transition region.

For the theory of Stark broadening this proves that line profiles may be obtained from the probability density and covariance of the plasma microfield alone, more complicated statistical features being insignificant in this context. Therefore the MMM offers a possibility to treat electron and ion broadening on a completely equal footing and to get rid of the static ion approximation underlying the unified theory. The results of an investigation of the effects of ion motion on hydrogen lines will be published separately.

Appendix A: Angular Averages

To begin with, let A_0 be any operator on $\mathfrak{H}^{(n)} \otimes \mathfrak{H}^{(\nu)}$ independent of Φ, and set

$$A(\Phi) = \exp\{-i\,\Phi\, l_z^{(n)}\} \otimes \exp\{i\,\Phi\, l_z^{(\nu)}\}\, A_0 \exp\{i\,\Phi\, l_z^{(n)}\} \otimes \exp\{-i\,\Phi\, l_z^{(\nu)}\}\,. \tag{A.1}$$

Then we have, since the $|\,l\,m\rangle$ and $|\,\lambda\,\mu\rangle$ are eigenstates of l_z :

$$\langle l\,m;\,\lambda\,\mu\,|\,A(\Phi)\,|\,l'\,m';\,\lambda'\,\mu'\rangle = \exp\{-i\,\Phi(m-\mu-m'+\mu')\}\langle l\,m;\,\lambda\,\mu\,|\,A_0\,|\,l'\,m';\,\lambda'\,\mu'\rangle\,, \tag{A.2}$$

and the average with respect to Φ yields

$$\langle l\,m;\,\lambda\,\mu\,|\,\langle A(\Phi)\rangle_\Phi\,|\,l'\,m';\,\lambda'\,\mu'\rangle = \delta_{m-\mu,\,m'-\mu'}\langle l\,m;\,\lambda\,\mu\,|\,A_0\,|\,l'\,m';\,\lambda'\,\mu'\rangle\,. \tag{A.3}$$

Thus $\langle \tilde{U}(\omega_e'\,|\,\boldsymbol{E}_i+\boldsymbol{E}_e)\rangle_{\Phi_e}$ and $\langle \tilde{U}_i(\omega_i'\,|\,\boldsymbol{E}_i)\rangle_{\Phi_i}$ possess this structure as has been claimed in Section 2.

Now take

$$A_0 = \exp\{-i\,\Theta_i\, l_y^{(n)}\} \otimes \exp\{-i\,\Theta_i\, l_y^{(\nu)}\}\,\tilde{U}_i(\omega_i'\,|\,E_i\,\boldsymbol{e}_z)\exp\{i\,\Theta_i\, l_y^{(n)}\} \otimes \exp\{i\,\Theta_i\, l_y^{(\nu)}\}\,. \tag{A.4}$$

Then the Θ_i-average results in

$$\begin{aligned}
&\langle l\,m;\,\lambda\,\mu\,|\,\langle A_0\rangle_{\Theta_i}\,|\,l'\,m';\,\lambda'\,\mu'\rangle\,\delta_{m-\mu,\,m'-\mu'}\\
&=\tfrac{1}{2}\sum\delta_{\tilde m-\tilde\mu,\,\tilde m'-\tilde\mu'}\,\langle\tilde l\,\tilde m;\,\tilde\lambda\,\tilde\mu\,|\,\tilde U_i(\omega_i'\,|\,E_i\,\boldsymbol{e}_z)\,|\,\tilde l'\,\tilde m';\,\tilde\lambda'\,\tilde\mu'\rangle\\
&\quad\cdot\int_0^\pi \mathrm{d}\Theta\,\sin\Theta\,\langle l\,m;\,\lambda\,\mu\,|\exp\{-i\,\Theta\,l_y^{(n)}\}\otimes\exp\{-i\,\Theta\,l_y^{(v)}\}\,|\,\tilde l\,\tilde m;\,\tilde\lambda\,\tilde\mu\rangle\\
&\qquad\cdot\langle\tilde l'\,\tilde m';\,\tilde\lambda'\,\tilde\mu'\,|\exp\{i\,\Theta\,l_y^{(n)}\}\otimes\exp\{i\,\Theta\,l_y^{(v)}\}\,|\,l'\,m';\,\lambda'\,\mu'\rangle\,\delta_{m-\mu,\,m'-\mu'}\\
&=\tfrac{1}{2}\sum\delta_{\tilde m-\tilde\mu,\,\tilde m'-\tilde\mu'}\,\langle l\,\tilde m;\,\lambda\,\tilde\mu\,|\,\tilde U_i(\omega_i'\,|\,E_i\,\boldsymbol{e}_z)\,|\,l'\,\tilde m';\,\lambda'\,\tilde\mu'\rangle\\
&\quad\cdot\int_0^\pi \mathrm{d}\Theta\,\sin\Theta\,r^{(l)}_{m\tilde m}(\Theta)\,r^{(\lambda)}_{\mu\tilde\mu}(\Theta)\,r^{(l')}_{\tilde m'm'}(-\Theta)\,r^{(\lambda')}_{\tilde\mu'\mu'}(-\Theta)\,\delta_{m-\mu,\,m'-\mu'}\,.
\end{aligned}\tag{A.5}$$

The first sum is with respect to $\tilde l$, $\tilde m$, $\tilde l'$, $\tilde m'$, $\tilde\lambda$, $\tilde\mu$, $\tilde\lambda'$, $\tilde\mu'$, but due to [29]

$$\langle l\,m\,|\exp\{-i\,\Theta\,l_y^{(n)}\}\,|\,\tilde l\,\tilde m\rangle=\delta_{l\tilde l}\,r^{(l)}_{m\tilde m}(\Theta)\tag{A.6}$$

the l-summations may be carried out and are no longer contained in the second sum. The additional Kronecker symbol results from the structure of $\tilde U_i(\omega_i'\,|\,E_i\,\boldsymbol{e}_z)$ which is the same as that of $\langle\tilde U(\omega_e'\,|\,\boldsymbol{E}_i+\boldsymbol{E}_e)\rangle_{\Phi_e}$. For the elements of the rotation matrices one has

$$r^{(l)}_{mm'}(-\Theta)=r^{(l)}_{m'm}(\Theta)\,,\tag{A.7}$$

and products of two of them may be reduced with the help of [29]

$$r^{(l)}_{m\tilde m}(\Theta)\,r^{(\lambda')}_{\mu'\tilde\mu'}(\Theta)=\sum_L\langle l\,\lambda'\,m\,\mu'\,|\,L\,m+\mu'\rangle\,\langle l\,\lambda'\,\tilde m\,\tilde\mu'\,|L\,\tilde m+\tilde\mu'\rangle\,r^{(L)}_{m+\mu',\,\tilde m+\tilde\mu'}(\Theta)\,.\tag{A.8}$$

Thus the integral in (A 5) becomes

$$\begin{aligned}
&\tfrac{1}{2}\int_0^\pi \mathrm{d}\Theta\,\sin\Theta\,r^{(l)}_{m\tilde m}(\Theta)\,r^{(\lambda)}_{\mu\tilde\mu}(\Theta)\,r^{(l')}_{\tilde m'm'}(-\Theta)\,r^{(\lambda')}_{\tilde\mu'\mu'}(-\Theta)\,\delta_{m-\mu,\,m'-\mu'}\,\delta_{\tilde m-\tilde\mu,\,\tilde m'-\tilde\mu'}\\
&=\tfrac{1}{2}\sum_{L,L'}\langle l\,\lambda'\,m\,\mu'\,|\,L\,m+\mu'\rangle\,\langle l\,\lambda'\,\tilde m\,\tilde\mu'\,|L\,\tilde m+\tilde\mu'\rangle\,\langle l'\,\lambda\,m'\,\mu|\,L'\,m'+\mu\rangle\,\langle l'\,\lambda\,\tilde m'\,\tilde\mu\,|\,L'\,\tilde m'+\tilde\mu\rangle\\
&\quad\cdot\int_0^\pi \mathrm{d}\Theta\,\sin\Theta\,r^{(L)}_{m+\mu',\,\tilde m+\tilde\mu'}(\Theta)\,r^{(L')}_{m'+\mu,\,\tilde m'+\tilde\mu}(\Theta)\,\delta_{m-\mu,\,m'-\mu'}\,\delta_{\tilde m-\tilde\mu,\,\tilde m'-\tilde\mu'}\,.
\end{aligned}\tag{A.9}$$

Due to the Kronecker symbols, the matrix elements of $r^{(L)}$ and $r^{(L')}$ on the right hand side have identical indices, so the orthogonality relation [30]

$$\tfrac{1}{2}\int_0^\pi \mathrm{d}\Theta\,\sin\Theta\,r^{(L)}_{m\tilde m}(\Theta)\,r^{(L')}_{m\tilde m}(\Theta)=(2\,L+1)^{-1}\,\delta_{LL'}\tag{A.10}$$

may be utilized. Taking all this together we find

$$\begin{aligned}
&\langle l\,m;\,\lambda\,\mu|\,\langle\tilde U_i(\omega_i'\,|\,\boldsymbol{E}_i)\rangle_{\Phi_i,\Theta_i}\,|\,l'\,m';\,\lambda'\,\mu'\rangle\\
&=\delta_{m-\mu,\,m'-\mu'}\sum_{\substack{\tilde m,\,\tilde m'\\ \tilde\mu,\,\tilde\mu'}}\delta_{\tilde m-\tilde\mu,\,\tilde m'-\tilde\mu'}\,\langle l\,\tilde m;\,\lambda\,\tilde\mu\,|\,\tilde U_i(\omega_i'\,|\,E_i\,\boldsymbol{e}_z)\,|\,l'\,\tilde m';\,\lambda'\,\tilde\mu'\rangle\\
&\quad\cdot\sum_L(2\,L+1)^{-1}\langle l\,\lambda'\,m\,\mu'\,|\,L\,m+\mu'\rangle\,\langle l\,\lambda'\,\tilde m\,\tilde\mu'\,|L\,\tilde m+\tilde\mu'\rangle\,\langle l'\,\lambda\,m'\,\mu\,|\,L\,m+\mu'\rangle\,\langle l'\,\lambda\,\tilde m'\,\tilde\mu|L\,\tilde m+\tilde\mu'\rangle\,.
\end{aligned}\tag{A.11}$$

Appendix B: Computation of $\tilde{\mathrm{W}}$

From (2.4), (2.5), and (2.8) we have

$$W(t\,|\,\boldsymbol{E})=\exp\{-i\,t\,\boldsymbol{E}\cdot\boldsymbol{r}^{(n)}\}\otimes\exp\{i\,t\,\boldsymbol{E}\cdot\boldsymbol{r}^{(v)}\}\,,\tag{B.1}$$

with $\boldsymbol{E}$ given by (2.7), that is $E_y=0$. The problem is to evaluate the operator exponentials. This might be accomplished by rotating $\boldsymbol{E}$ into the z-axis, taking matrix elements in a basis of "parabolic" states [19], and

rotating back again. Here we shall prefer another straightforward approach. The eigenvalues of $\boldsymbol{E}\cdot\boldsymbol{r}^{(n)}$ are

$$-\tfrac{3}{2}n(n-1)E\,,\quad -\tfrac{3}{2}n(n-2)E\,,\ldots,\quad \tfrac{3}{2}n(n-1)E\,, \tag{B.2}$$

and $\boldsymbol{E}\cdot\boldsymbol{r}^{(n)}$ is a Hermitian operator, so we may employ the Lagrange-Sylvester interpolation polynomial [31] to obtain

$$\exp\{-i\,t\,\boldsymbol{E}\cdot\boldsymbol{r}^{(n)}\}=\sum_{k=1-n}^{n-1}\exp\{-\tfrac{3}{2}\,i\,k\,n\,E\,t\}\prod_{\substack{m=1-n\\ m\neq k}}^{n-1}\frac{\dfrac{2}{3\,n\,E}\,\boldsymbol{E}\cdot\boldsymbol{r}^{(n)}-m}{k-m}. \tag{B.3}$$

The products are polynomials of degree $2(n-1)$ in $E^{-1}\,\boldsymbol{E}\cdot\boldsymbol{r}^{(n)}$:

$$\prod_{\substack{m=1-n\\ m\neq k}}^{n-1}\frac{\dfrac{2}{3\,n\,E}\,\boldsymbol{E}\cdot\boldsymbol{r}^{(n)}-m}{k-m}=\sum_{m=0}^{2(n-1)}a_{mk}^{(n)}\,(\tfrac{3}{2}n)^{-m}\,(E^{-1}\,\boldsymbol{E}\cdot\boldsymbol{r}^{(n)})^{m}\,, \tag{B.4}$$

with coefficients $a_{mk}^{(n)}$ for which it is easily shown that

$$a_{m,-k}^{(n)}=(-)^{m}\,a_{mk}^{(n)}\,,\quad a_{2m-1,k}^{(n)}=k\,a_{2m,k}^{(n)}\,. \tag{B.5}$$

Because of $E_y=0$ we have

$$(\boldsymbol{E}\cdot\boldsymbol{r}^{(n)})^{m}=(E_x\,x^{(n)}+E_z\,z^{(n)})^{m}=:\sum_{l=0}^{m}v_{ml}^{(n)}\,E_x^{m-l}\,E_z^{l}\,. \tag{B.6}$$

The $v_{ml}^{(n)}$ defined by (B. 6) are built from products of $x^{(n)}$ and $z^{(n)}$, and hence have real matrix elements between angular momentum eigenstates. (Note that $x^{(n)}$ and $z^{(n)}$ do not commute though x and z do!) Insertion into (B. 3) yields

$$\exp\{-i\,t\,\boldsymbol{E}\cdot\boldsymbol{r}^{(n)}\}=\sum_{m=0}^{2(n-1)}(\tfrac{3}{2}\,n)^{-m}\sum_{k=1-n}^{n-1}a_{mk}^{(n)}\sum_{l=0}^{m}v_{ml}^{(n)}\,E_x^{m-l}\,E_z^{l}\,E^{-m}\,\exp\{-\tfrac{3}{2}\,i\,k\,n\,E\,t\}\,, \tag{B.7}$$

and $\exp(i\,t\,\boldsymbol{E}\cdot\boldsymbol{r}^{(\nu)})$ is just the same with ν instead of n and $-t$ instead of t. But then

$$W(t\,|\,\boldsymbol{E})=\sum_{M=0}^{2(n+\nu-2)}\sum_{L=0}^{M}\sum_{N}\tilde{K}_{LMN}^{(n,\nu)}\,E_x^{M-L}\,E_z^{L}\,E^{-M}\,\exp\{-\tfrac{3}{2}\,i\,N\,E\,t\} \tag{B.8}$$

with the $\tilde{K}$-matrices defined by

$$\tilde{K}_{LMN}^{(n,\nu)}\sum_{m=0}^{2n-2}\sum_{\mu=0}^{2\nu-2}\sum_{l=0}^{m}\sum_{\lambda=0}^{\mu}\sum_{k=1-n}^{n-1}\sum_{\varkappa=1-\nu}^{\nu-1}\delta_{M,\,m+\mu}\,\delta_{L,\,l+\lambda}\,\delta_{N,\,nk-\nu\varkappa}\,(\tfrac{2}{3})^{M}\,n^{-m}\,\nu^{-\mu}\,a_{mk}^{(n)}\,a_{\mu\varkappa}^{(\nu)}\,v_{ml}^{(n)}\otimes v_{\mu\lambda}^{(\nu)}\,. \tag{B.9}$$

N is the "quantum number" characterizing the Stark components in a static electric field. With the help of (B. 5) it may be shown that

$$\tilde{K}_{LM-N}^{(n,\nu)}=(-)^{M}\,\tilde{K}_{LMN}^{(n,\nu)} \tag{B.10}$$

holds, so that (B 8) is the same as

$$\begin{aligned}W(t\,|\,\boldsymbol{E})=&\sum_{m=0}^{n+\nu-2}\sum_{L=0}^{2m}\sum_{N\geq 0}K_{L\,2m\,N}^{(n,\nu)}\,E_x^{2m-L}\,E_z^{L}\,E^{-2m}\cos(\tfrac{3}{2}\,N\,E\,t)\\&-i\sum_{m=0}^{n+\nu-3}\sum_{L=0}^{2m+1}\sum_{N>0}K_{L\,2m+1\,N}^{(n,\nu)}\,E_x^{2m+1-L}\,E_z^{L}\,E^{-2m-1}\sin(\tfrac{3}{2}\,N\,E\,t)\end{aligned} \tag{B.11}$$

with $K_{LMN}^{(n,\nu)}:=(2-\delta_{0,N})\,\tilde{K}_{LMN}^{(n,\nu)}$.

Now consider a rotation of angle π around the z-axis. The only bearing this has on the right hand side of (B. 11) is to change the sign of E_x. For this reason, only those terms containing even powers of E_x survive

the Φ_e-average to follow. But

$$E_x^{2(m-l)} = \sum_{k=0}^{m-l} (-)^k \binom{m-l}{k} E_z^{2k} E^{2(m-l-k)}, \tag{B.12}$$

which may be inserted into (B. 11). Then changing the order of summations this becomes

$$\begin{aligned} W(t|\boldsymbol{E}) = & \sum_{N\geq 0} \cos\left(\tfrac{3}{2} N E t\right) \sum_{k=0}^{n+\nu-2} \left(\frac{E_z}{E}\right)^{2k} \sum_{m=k}^{n+\nu-2} \sum_{l=0}^{k} (-)^{k+l} \binom{m-l}{k-l} K^{(n,\nu)}_{2l,2m,N} \\ & - i \sum_{N>0} \sin\left(\tfrac{3}{2} N E t\right) \sum_{k=0}^{n+\nu-3} \left(\frac{E_z}{E}\right)^{2k+1} \sum_{m=k}^{n+\nu-3} \sum_{l=0}^{k} (-)^{k+l} \binom{m-l}{k-l} K^{(n,\nu)}_{2l+1,2m+1,N} \\ & + \text{remainder}, \end{aligned} \tag{B.13}$$

the remainder vanishing under the average over Φ_e.

Defining the double sums which are the coefficients of $(E_z/E)^l$ as $H^{(n,\nu)}_{lN}$, and taking the Laplace transform, one arrives at (2.11).

[1] P. W. Anderson, J. Phys. Soc. Japan **9,** 316 [1954].
[2] R. Kubo, J. Phys. Soc. Japan **9,** 935 [1954].
[3] A. Brissaud and U. Frisch, JQSRT **11,** 1767 [1971].
[4] A. Brissaud and U. Frisch, J. Math. Phys. **15,** 524 [1974].
[5] A. Brissaud, C. Goldbach, J. Léorat, A. Mazure, and G. Nollez, J. Phys. B **9,** 1129 [1976].
[6] A. Brissaud, C. Goldbach, J. Léorat, A. Mazure, and G. Nollez, J. Phys. B **9,** 1147 [1976].
[7] D. Voslamber, Z. Naturforsch. **24 a,** 1458 [1969].
[8] E. W. Smith, J. Cooper, and C. R. Vidal, Phys. Rev. **185,** 140 [1969].
[9] C. R. Vidal, J. Cooper, and E. W. Smith, Astrophys. J. Suppl. **25,** 37 [1973].
[10] M. Baranger, in: Atomic and Molecular Processes (ed. by D. R. Bates), Academic Press, New York 1962.
[11] H. R. Griem, Plasma Spectroscopy, McGraw-Hill, New York 1964.
[12] H. R. Griem, Spectral Line Broadening by Plasmas, Academic Press, New York 1974.
[13] E. W. Smith, C. R. Vidal, and J. Cooper, J. Res. Nat. Bur. Stand. **73 A,** 389 [1969].
[14] E. W. Smith, J. Cooper, W. R. Chappell, and T. Dillon, JQSRT **11,** 1547 [1971].
[15] R. Lee, J. Phys. B **4,** 1640 [1971].
[16] J. Seidel, Dissertation, Universität Düsseldorf 1974 (unpublished).
[17] D. R. Cox, Renewal Theory, Methuen, London 1962.
[18] D. C. Montgomery, Theory of the Unmagnetized Plasma, Gordon and Breach, New York 1971.
[19] H. A. Bethe and E. E. Salpeter, Quantum Mechanics of One- and Two-Electron Atoms, Springer, Berlin 1957.
[20] M. Baranger and B. Mozer, Phys. Rev. **115,** 521 [1959].
[21] B. Mozer and M. Baranger, Phys. Rev. **118,** 626 [1960].
[22] H. Pfennig and E. Trefftz, Z. Naturforsch. **21 a,** 697 [1966].
[23] C. F. Hooper, Phys. Rev. **149,** 77 [1966].
[24] C. F. Hooper, Phys. Rev. **165,** 215 [1968].
[25] W. R. Chappell, J. Cooper, and E. W. Smith, JQSRT **10,** 1195 [1970].
[26] L. J. Roszman, Phys. Rev. Lett. **34,** 785 [1975].
[27] W. L. Wiese, D. E. Kelleher, and V. Helbig, Phys. Rev. A **11,** 1854 [1975].
[28] W. L. Wiese, D. E. Kelleher, and D. R. Paquette, Phys. Rev. A **6,** 1132 [1972].
[29] A. Messiah, Quantum Mechanics, Vol. II, North-Holland, Amsterdam 1965.
[30] A. R. Edmonds, Angular Momentum in Quantum Mechanics, Princeton UP, Princeton 1960.
[31] M. C. Pease, Methods of Matrix Algebra, Academic Press, New York 1965.